THE JOURNAL OF BIOLOGICAL CHEMISTRY Vol. 272, No. 48, Issue of November 28, pp. 30552–30557, 1997
Printed in U.S.A.

Topology of NAT2, a Prototypical Example of a New Family of Amino Acid Transporters*

(Received for publication, June 27, 1997, and in revised form, September 17, 1997)

Hui-Chu Chang‡ and Daniel R. Bush‡§¶

From the ‡Department of Plant Biology, University of Illinois at Urbana-Champaign and the §Photosynthesis Research Unit, United States Department of Agriculture, Agricultural Research Service, University of Illinois, Urbana, Illinois 61801

Amino acids are the predominant form of nitrogen available to the heterotrophic tissues of plants. These essential organic nutrients are transported across the plasma membrane of plant cells by proton-amino acid symporters. Our lab has cloned an amino acid transporter from *Arabidopsis*, NAT2/AAP1, that represents the first example of a new class of membrane transporters. We are investigating the structure and function of this porter because it is a member of a large gene family in plants and because its wide expression pattern suggests it plays a central role in resource allocation. In the results reported here, we investigated the topology of NAT2 by engineering a c-*myc* epitope on either the N or C terminus of the protein. We then used *in vitro* translation, partial digestion with proteinase K, and immunoprecipitation to identify a group of oriented peptide fragments. We modeled the topology of NAT2 based on the lengths of the peptide fragments that allowed us to estimate the location of protease accessible cleavage sites. We independently identified the location of the N and C termini using immunofluorescence microscopy of NAT2 expressed in COS-1 cells. We also investigated the glycosylation status of several sites of potential *N*-linked glycosylation. Based on the combined data, we propose a novel 11 transmembrane domain model with the N terminus in the cytoplasm and C terminus facing outside the cell. This model of protein topology anchors our complementary investigations of porter structure and function using site-directed and random mutagenesis.

Amino acids are actively transported into plant cells by proton-coupled symporters (1). These proteins link translocation across the plasma membrane to the proton-motive force generated by a P-type, H^+-ATPase (2, 3). In plants, there are many heterotrophic tissue systems that are dependent upon carbon and nitrogen import for growth and development. Since amino acids are the primary form of nitrogen available to the heterotrophic plant tissues, the amino acid symporters are responsible for the systemic distribution of organic nitrogen, and therefore, they are essential contributors to plant growth (4, 5). Detailed investigations of the transport properties and bioenergetics of these symporters using isolated plasma membrane vesicles and imposed proton electrochemical potential differences have shown that they are electrogenic transporters that are driven by either transmembrane proton or electrical potential differences (6). These transporters are inhibited by chemical modification of histidine residues by diethyl pyrocarbonate (6), and substrate protection experiments suggest the sensitive residue is at or near the substrate binding site (5, 7). Several classes of symporters were initially resolved based on expression patterns and substrate specificity (6, 8–11). Transport competition experiments showed that binding sites are stereospecific and identified the carboxylic acid, the alpha amino group, and substitutions at the β-carbon as important determinants in governing substrate binding (8, 9). Recently, one of these symporters was expressed in *Xenopus* oocytes, and electrophysiological methods allowed for a high resolution investigation of transport kinetics that suggests these transporters operate by a simultaneous binding mechanism (12).

The first plant amino acid symporter cloned (NAT2/AAP1) was identified by two groups using functional complementation of yeast amino acid transport mutants with different *Arabidopsis* cDNA expression libraries (13, 14). The deduced amino acid sequence of the encoded protein contains 485 amino acid residues with a calculated molecular mass of 52.9 kDa and three sites of potential *N*-linked glycosylation. Hydropathy analysis suggested this is an integral membrane protein with 10–12 membrane-spanning regions. A search of the non-redundant protein data bases did not identify any strong homologies, suggesting NAT2/AAP1 represented a new class of transport protein (13).

Several amino acid transporter genes have now been isolated from *Arabidopsis* using functional complementation of yeast transport mutants (15). These include five clones that are closely related to NAT2/AAP1 (AAP2–6) (16–18), a cationic amino acid transporter (AAT1) (19), two proline transporters (ProT1 and ProT2) (18), and a lysine and histidine transporter (LHT1) (20). Most of the plant amino acid transporters have relatively broad substrate specificity although they often exhibit some preference (lower K_m or higher V_{max}) for related groups of amino acids. The presence of multiple genes coding for amino acid carriers suggests there is considerable complexity in the function of these transporters in nitrogen allocation in plants (21).

Despite the physiological importance of amino acid transporters in plant growth, little is known about these transport proteins at the molecular level. This deficiency is a result of the difficulty of working with low abundance membrane proteins and the apparent toxicity of these eukaryotic membrane proteins expressed in *E. coli*.[1] To learn more about the molecular structure and function of plant amino acid symporters, our laboratory has chosen NAT2/AAP1 as a prototypical example for detailed analysis. We chose this symporter because it is a

* The costs of publication of this article were defrayed in part by the payment of page charges. This article must therefore be hereby marked "*advertisement*" in accordance with 18 U.S.C. Section 1734 solely to indicate this fact.

¶ To whom correspondence should be addressed: USDA-ARS and Dept. of Plant Biology, University of Illinois at Urbana-Champaign, 196 ERML, 1201 W. Gregory Dr., Urbana, IL 61801. Tel.: 217 333 6109; Fax: 217 244 4419; E-mail: dbush@uiuc.edu.

[1] T.-J. Chiou and D. R. Bush, unpublished data.

member of a large family of translocators, because it transports amino acids that are commonly found in the phloem translocation stream, and also because it is widely expressed in plant tissues, suggesting it plays an important role in nitrogen partitioning. In the results reported here, we have investigated the topology of NAT2 in the plasma membrane as an important first step in describing plant amino acid symporters at the molecular level. We determined its membrane topology by engineering a c-*myc* epitope onto the N or C terminus, and then we expressed the chimeric proteins in a cell-free translation system, in yeast, and in COS-1 cells.

EXPERIMENTAL PROCEDURES

Chimeric Gene Constructs—Arabidopsis NAT2 cDNA was digested with *Eco*RI, and the 1.7-kb fragment was subcloned into pBSks(+) vector under the T7 promoter to produce plasmid pBS-NAT2. An *Nde*I site was engineered at the nucleotide 1530 of NAT2 cDNA by site-directed mutagenesis. The site-directed mutagenesis was carried out according to the Bio-Rad manual (No. 170–3581) based on the method of Kunkel (22). The *in vitro* synthesis of the mutant DNA strand was performed by using the uracil-containing single-stranded DNA from plasmid pBS-NAT2 grown in *Escherichia coli* strain CJ236 as template with the oligonucleotide 5′-TCCGGACTATGCATATGTGAGTTT-GAGATC-3′ as primer. The pBS-NAT2/*Nde*I plasmids were transformed into *E. coli* strain DH5α (Life Technologies, Inc.), and the transformants were screened on the ampicillin LB plates and confirmed by DNA sequencing. A human c-*myc* epitope cassette was acquired that contains six repeats of MEQKLISEEDLNQ (the epitope is *underlined*). This epitope is recognized by monoclonal antibody, Myc1–9E10 (23). The 6x *myc* cassette in the vector pGEM7z(+) was kindly provided by Dr. N. Raikhel (Michigan State University). To construct the *myc* epitope on the C terminus of NAT2, the 6x *myc* cassette was amplified by polymerase chain reaction with two primers, 5′-ATCGATTTAAA-CATATGG-3′ and 5′-GGGGTATCTAGATCAAGT-3′, which contain an *Nde*I site and an *Xba*I site, respectively. The *Nde*I/*Xba*I polymerase chain reaction fragment was subcloned into pBS-NAT2/*Nde*I by *Nde*I and *Xba*I to produce plasmid pBS-6C. To construct the *myc* epitope on the N terminus of NAT2, an *Eco*RI site was engineered at the nucleotide position 89 on NAT2 cDNA of pBS-NAT2 by site-directed mutagenesis. The site-directed mutagenesis was performed with the primer 5′-CT-CATCACTATGAATTCGAGTTTCAACACAG-3′. The *Eco*RI fragment of NAT2/*Eco*RI mutant was subcloned into pGEM7z with 6x *myc* cassette on the 5′-end of the epitope cassette to produce plasmid pGEM-6N. For yeast expression, both the C- and N-*myc*-tagged NAT2 cDNAs were subcloned into pNEV-E, a yeast/*E. coli* shuttle vector with 2 μ-based replication origin (24). For COS-1 cells expression, the epitope-tagged NAT2 constructs were subcloned into a mammalian expression vector, pCMV5 (25). The plasmid pCMV5–6C was constructed by inserting *Kpn*I-*Bam*HI fragment of pBS-6C into the *Kpn*I-*Bam*HI site of pCMV5. The plasmid pCMV5–6N was constructed by inserting *Eco*RI fragment of pGEM-6N into the *Eco*RI site of pCMV5, and the orientation of insert DNA was checked by *Pst*I digestion. All DNA manipulations were conducted according to the standard protocols (26), unless specified. The DNA sequence of all mutants and ligation products were confirmed by the dideoxy chain-termination method (27) using Sequenase Version 2.0 (U. S. Biochemical Corp.).

Yeast Growth and Transformation—The strain of *Saccharomyces cerevisiae* used in this study was JT16 (*MATa hip1–614 his4–401 ura3–52 ino1 can1*) (28). JT16 was maintained on complete yeast extract/peptone/dextran medium supplemented with 650 μM histidine at 30 °C. Ura^+ transformants were selected on S1 medium, which contains 2% glucose, 0.17% yeast nitrogen base (without amino acid and ammonium sulfate), 0.5% ammonium sulfate, 0.002% inosine, 0.1% arginine, and supplemented with histidine. For high histidine $(HH)^2$ medium, 3.9 mM histidine was supplemented to S1 medium; for low histidine (LH) medium, 130 μM histidine was included (13). Yeast JT16 cells were transformed with *myc*-tagged NAT2 cDNA-containing plasmids by electroporation (29). Electroporated cells were collected on HH or LH medium with 1 M sorbitol. Stable transformants of pNEV-E were grown on HH medium; NAT2, C-tagged, and N-tagged NAT2 transformants were maintained on LH medium.

Amino Acid Transport Assay in Yeast—Uptake of [^{14}C]alanine was examined as described previously (13). The transport solution contained 2% glucose, 0.17% yeast nitrogen base (without amino acid and ammonium sulfate), 0.5% ammonium sulfate, pH 5.0, 0.1 mM alanine, and 0.2 μCi of [^{14}C]alanine (152 μCi/mmol). For kinetic analysis, alanine concentrations of 0.1, 0.2, 0.4, 0.6, 1.0, and 2.0 mM were used. Cells were collected at the desired time points on micropore filters, and accumulated radioactivity was measured by scintillation spectroscopy. All transport measurements were repeated three times with duplicate samples included for each treatment.

In Vitro Transcription and Translation—The *in vitro* transcription and translation reactions were carried out in the Promega TNT reticulocyte lysate coupled system, with or without microsomal membranes, according to the manufacturer instructions. Microsomes were isolated from hen oviducts according to the method described by Lively and Walsh (30). Briefly, the magnum portion of chicken oviduct was homogenized, and the membrane fraction was separated by step sucrose gradient in Beckman SW-28 rotor for 16 h at 100,000 × *g*. The band between the 1.5 and 2.0 M sucrose layers was collected and treated with 15 mM EDTA. The EDTA-treated membranes were pelleted and then resuspended in 20 mM HEPES, pH 7.5, 0.25 M sucrose, and 2 mM dithiothreitol to a concentration of 50–70 A_{280} units/ml, and aliquots were stored at −80 °C. For each *in vitro* transcription/translation reaction, 1 μg of pBS-NAT2, pBS-6C, or pGEM-6N was added. The reticulocyte lysate, amino acids, T3 or T7 RNA polymerase, [^{35}S]methionine and [^{35}S]cysteine (Tran^{35}S-label, ICN Radiochemicals), and EDTA-treated rough microsomes were added according to the manufacturer instructions. After incubation at 30 °C for 90 min, the reaction was terminated, and the products were ready for further analysis. Alkaline extraction was used to show the porter was incorporated in the microsomes. An equal volume of 0.2 M sodium carbonate (pH 11.0) was added to the finished *in vitro* translation reactions and incubated on ice for 30 min. Microsomes were pelleted with 150,000 × *g* centrifugation for 30 min, then supernatant and pellet proteins were separated with SDS-PAGE, and radioactive bands were visualized by fluorography using EN^{3}HANCE (NEN Life Science Products).

Proteinase K Digestion and Immunoprecipitation—The *in vitro* translation reactions were centrifuged at 150,000 × *g* for 30 min. The membrane pellets were washed with TE buffer (10 mM Tris, pH 7.6, and 1 mM EDTA) and repelleted. Washed membranes were resuspended in ice-cold TE with proteinase K (20 μg/ml). Proteolysis proceeded on ice for 10–60 min in the presence or absence of 1% Triton X-100 and was stopped by adding 500 μl of cold RIPA (10 mM Tris-HCl, pH 7.6, 0.15 M NaCl, 1% sodium deoxycholate, 1% Triton X-100, 0.1% SDS, 1 mM EDTA, and 1 mM phenylmethylsulfonyl fluoride). The proteolytic peptides were collected by immunoprecipitation with Myc1–9E10 monoclonal antibody. Immunoprecipitation was carried out according to the method described by Szczesna-Skorupa and Kemper (31). After incubation with antibody overnight, 50 μl of protein A-Sepharose slurry (40 mg/ml) (CL-4B, Pharmacia Biotech Inc.) was added to the immunoprecipitates and incubated for an additional hour. After washing with RIPA buffer and TSA buffer (10 mM Tris-HCl, pH 7.6, 0.15 M NaCl, and 1 mM EDTA), immunoprecipitated proteins were eluted by heating at 65 °C for 10 min in SDS gel loading buffer. Proteins were separated on 12% gels with SDS-PAGE and visualized by fluorography.

Transfection of COS-1 Cells—COS-1 cells were maintained at 37 °C with 6% CO_2 in Dulbecco's modified Eagle's medium (DMEM) (Life Technologies, Inc.), supplemented with 10% calf serum (Sigma) and 100 units/ml penicillin and 0.1 mg/ml streptomycin (Life Technologies, Inc.). At 80% confluence, COS-1 cells were transfected in 35-mm culture dishes with the expression vector pCMV5 containing epitope-tagged NAT2 cDNAs or with pCMV5 vector only as mock cells. 0.1 ml of DMEM containing 2 μg of DNA was mixed with same amount of DMEM with 5 μl of Lipofectin (Life Technologies, Inc.) and incubated for 30 min at room temperature, and 0.8 ml of DMEM was added to the mixture and placed on COS-1 cells. After incubation for 4 h, the transfection mixture was aspirated and replaced with DMEM with 10% calf serum. Cells were grown in medium for 48 h before ^{35}S-protein labeling or immunofluorescent staining.

In Vivo Labeling of COS-1 Cell Proteins and Immunoprecipitation—COS-1 cells were grown and transfected in 35-mm dishes for radiolabeling of recently synthesized proteins (31). 48 h after transfection, cells were pre-incubated for 30 min in methionine- and cysteine-free DMEM. Cells were then labeled for 2 h with the same medium containing 120 μCi/ml of [^{35}S]methionine and [^{35}S]cysteine (Tran^{35}S-label, ICN Radiochemicals). After labeling, cells were washed twice with ice-cold PBS

[2] The abbreviations used are: HH, high histidine; LH, low histidine; PAGE, polyacrylamide gel electrophoresis; DMEM, Dulbecco's modified Eagle's medium; PBS, phosphate-buffered saline; FITC, fluorescein isothiocyanate; TMD, transmembrane domain; ER, endoplasmic reticulum.

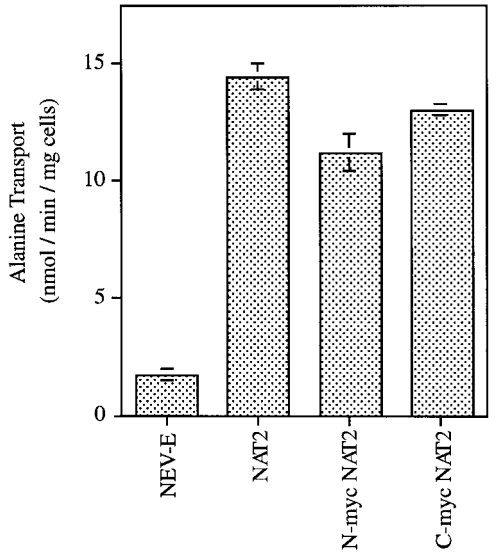

FIG. 1. **Alanine transport in yeast JT16.** Alanine transport into JT16 transformed with NEV-E (insert-free vector as control), N-myc NAT2 (*myc* tagged on the N terminus of NAT2), or C-myc NAT2 (*myc* tagged on the C terminus of NAT2) was measured. The transport solution contained 0.1 mM alanine and 0.2 μCi of [^{14}C]alanine (152 mCi/mmol). Each experiment was repeated three times with duplicates for each treatment.

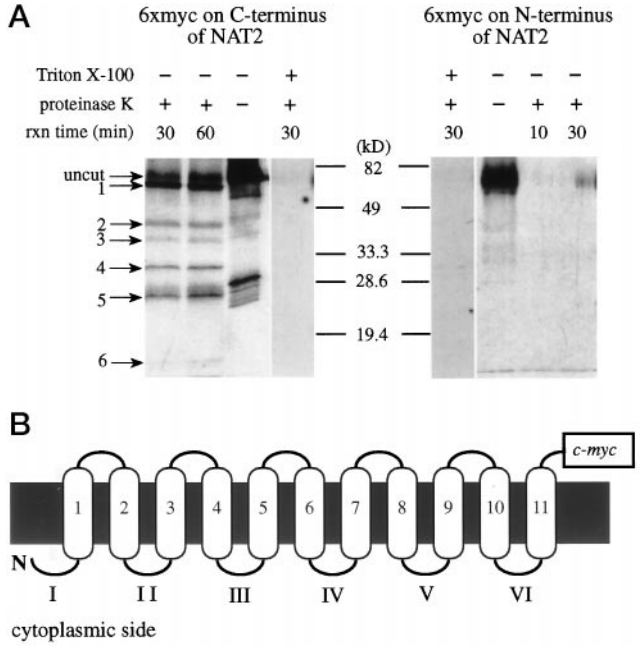

FIG. 2. **Immunoprecipitation of epitope-tagged NAT2 after partial proteolysis and the proposed topology model.** *A*, the *myc*-tagged NAT2 proteins were expressed in a cell-free translation system with ER-derived microsomal membranes followed by proteolysis with 20 μg/ml of proteinase K on ice for 10–60 min in the presence or absence of 1% Triton X-100. Proteolytic products were immunoprecipitated with human Myc1–9E10 monoclonal antibody, followed with SDS-PAGE and visualized by fluorography. The tagged protein migrates at $\approx$ 60 kDa. *B*, topology model proposed from partial proteolysis. The *myc* tag on the C terminus of NAT2 was protected by the membrane, and partial proteolysis generated six small peptides. *Band 1* represents the proteolytic product cut at *loop I*; *band 2* is the product cut at *loop II*, and so on.

(phosphate-buffered saline) and lysed in 0.5 ml of RIPA buffer for 10 min on ice. Lysates were clarified by centrifugation for 15 min in a microfuge. Immunoprecipitation with mouse anti-human Myc1–9E10 antibody was carried out as described above. Immunoprecipitated proteins were analyzed by SDS-PAGE and fluorography.

Immunofluorescent Staining—Indirect immunofluorescence was performed according to the method of Szczesna-Skorupa and Kemper (31). Briefly, COS-1 cells were grown on coverslips in 35-mm Petri dishes and transfected as described. After 48 h, cells were washed twice with PBS and fixed with 2.5% paraformaldehyde for 20 min. Cells were directly incubated with antibody or permeabilized with 0.1% Triton X-100 for 5 min followed by washing with 0.1% gelatin in PBS. Incubation with Myc1–9E10 monoclonal antibody was carried out for 40 min at room temperature followed by a 30-min incubation of a secondary antibody, fluorescein isothiocyanate (FITC)-conjugated goat anti-mouse IgG (Jackson Immunoresearch Laboratories). Cells were washed with 0.1% gelatin in PBS between incubation of antibodies. Cells were observed and photographed using Zeiss photomicroscope III equipped with epi-illumination optics and an HBO 100-watt mercury lamp.

RESULTS

Expression of myc-tagged NAT2 in Yeast—Chimeric NAT2 proteins were constructed with either an N- or C-terminal human *myc* epitope cassette (containing six copies of the *myc* epitope in series) as N-myc NAT2 and C-myc NAT2. The *myc*-tagged genes were subcloned into a yeast/*E. coli* shuttle vector, pNEV-E (24). Expression in yeast was driven by PMA1 (yeast plasma membrane H^+-ATPase), a strong constitutive promoter. Both of the *myc*-tagged NAT2 constructs were able to complement JT16, a histidine transport mutant, grown on low histidine medium suggesting the epitope-tagged proteins were still functional. Amino acid transport activity was measured directly with ^{14}C-labeled substrate, and the results showed that the C-myc NAT2 maintained 89% and N-myc NAT2 has 78% of the transport activity of wild-type NAT2 (Fig. 1). In addition, the K_m for alanine for the three proteins was not significantly different (105 $\pm$ 17 μM). These data show that epitope tagging did not interfere with transporter function and suggest the overall protein structure was maintained. Thus, these chimeric proteins were suitable for the following topological studies.

Expression of myc-Tagged NAT2 in a Cell-free Translation System and Partial Proteolysis—To study the topology of NAT2, the epitope-tagged proteins were expressed *in vitro* and investigated with partial proteolysis and immunoprecipitation. The *myc*-tagged NAT2 proteins were expressed in a cell-free translation system in the presence of microsomes. Alkaline extraction of the microsomes after *in vitro* translation showed that $\geq$ 50% of the translated protein was incorporated in the microsome membranes (data not shown). After *in vitro* co-translation, samples were treated on ice with 20 μg/ml proteinase K for 10–60 min, and then the proteolytic fragments were collected by immunoprecipitation with Myc1–9E10 monoclonal antibody. The precipitated peptides were separated with SDS-PAGE and visualized with fluorography (Fig. 2*A*). The rationale behind this experiment is that hydrophilic loops of NAT2 protein that are on the cytoplasmic side of the microsomal membrane are exposed to the protease while transmembrane domains and peptide loops on the luminal side of the microsome are protected from proteolysis. The N-myc NAT2 was not detected after 10 min of proteolysis, suggesting the N-terminal epitope was degraded by proteinase K (Fig. 2*A*). The resulting proteolytic fragments could not be immunoprecipitated with anti-*myc* antibody because they lacked the N-terminal *myc* epitope. These results are consistent with the N terminus of NAT2 facing the cytoplasmic side of the microsome. In contrast, the C-terminal *myc* epitope was not sensitive to proteinase K, suggesting the C terminus of NAT2 was located on the luminal side of the microsomal membrane vesicle (Fig. 2*A*). Moreover, proteolysis of C-myc NAT2 generated six peptide fragments of decreasing molecular mass that retained the C-terminal tag and were precipitable by the anti-*myc* antibody (Fig. 2*A*). When proteolysis was performed in the presence of Triton X-100, no protein fragments were detectable, which is

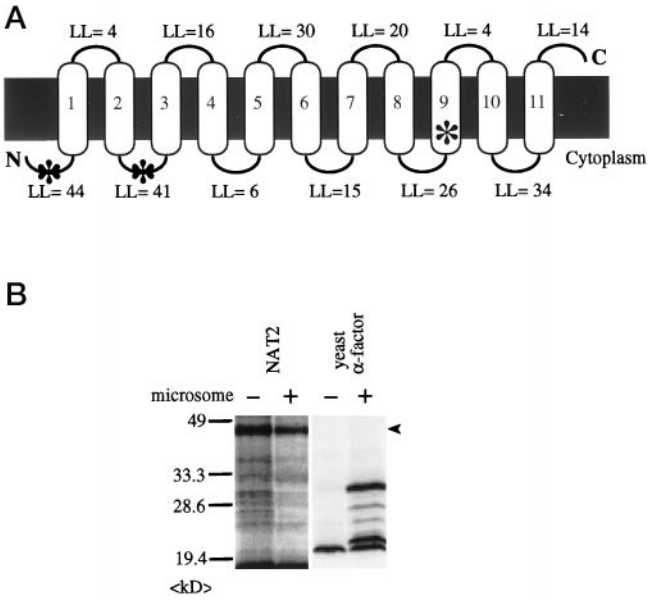

FIG. 3. **In vitro glycosylation study of NAT2 protein.** *A*, topology model of NAT2. There are three sites of potential *N*-linked glycosylation in NAT2 at the 10th, 105th, and 382nd amino acid residues. According to our proposed topology model, they are located in a transmembrane domain or the cytoplasmic face of the plasma membrane. Three potential glycosylation sites are marked (*). *LL*, loop length. *B*, NAT2 and yeast α-factor were expressed in the rabbit reticulocyte lysate with or without ER-enriched microsomal membranes. The expressed proteins were separated with SDS-PAGE and visualized by fluorography. Without microsomes, the molecular mass of NAT2 on SDS-PAGE was about 45 kDa, and yeast α-factor, a glycoprotein, was about 20 kDa.

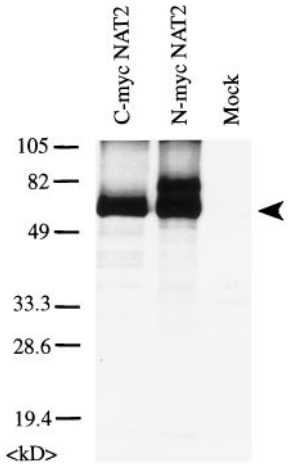

FIG. 4. **Immunoprecipitation of *myc*-tagged NAT2 expressed in COS-1 cells.** N- or C-*myc*-tagged NAT2 were expressed in COS-1 cells with a mammalian expression vector, pCMV5. Cells were labeled with [^{35}S]methionine and cysteine and lysed, and tagged NAT2 proteins were immunoprecipitated with Myc1–9E10 monoclonal antibody. Immunoprecipitated proteins were separated with SDS-PAGE and visualized by fluorography.

consistent with the notion that protease-resistant peptides were protected by the membrane. The lower molecular weight products observed in the absence of proteolysis are distinct from the proteolytic fragments and may be due to internal initiation of translation. The size of the C-terminal-tagged proteolytic products enabled us to estimate the approximate cleavage sites of proteinase K. Since proteinase K is not membrane-permeable, hydrolysis is dependent on the accessibility of loop regions of the peptide that exist between adjacent transmembrane domains. Thus, band 1 represents cleavage at loop I and band 2 at loop II and so on (Fig. 2*B*). The approximate molecular mass and the number of fragments produced with proteinase K are consistent with the six loop domains depicted in Fig. 2*B*.

Computer-generated models of NAT2 topology that consider hydrophobicity and the positive inside rule predict 10 or 11 membrane-spanning regions (32). The estimated length of the proteolytic fragments resulting from proteinase K digestion are consistent with the 11 transmembrane domain (TMD) model. Based on differential sensitivity of the *myc* epitopes to proteolysis, the size and number of proteolytic fragments, and the computer prediction, we propose that NAT2 protein contains 11 membrane-spanning regions, with the N terminus in the cytoplasm and C terminus facing outside the cell (Fig. 2*B*).

According to our model of NAT2 topology, three sites of potential *N*-linked glycosylation are not on the outside face of the plasma membrane (Fig. 3*A*). Therefore, these sites would not be exposed to the luminal side of the ER during protein synthesis and they should not be glycosylated. To test this hypothesis, NAT2 was expressed in rabbit reticulocyte lysate in the presence or absence of rough ER-enriched microsomal membranes. The apparent size of wild-type NAT2 on SDS-PAGE is about 45 kDa, which is smaller than its predicted molecular weight (52.9 kDa) but is typical of membrane protein mobility (33). NAT2 protein had the same mobility on SDS-PAGE in the presence or absence of microsomes, suggesting it was not glycosylated (Fig. 3*B*). As a positive control, the yeast α-factor exhibited a mobility shift due to glycosylation when co-translated with microsomes (Fig. 3*B*). The absence of glycosylation for NAT2 supports the 11 transmembrane domain model.

Expression and Immunofluorescent Staining in COS-1 Cells—To test the 11 transmembrane domain model independently, we expressed *myc*-tagged NAT2 proteins in COS-1 cells. The cells were labeled with [^{35}S]methionine/cysteine and then immunoprecipitated with c-*myc* antibody followed by SDS-PAGE and fluorography (Fig. 4). Both N- and C-terminal tagged proteins exhibited the same molecular weight as they did in the *in vitro* system, thereby demonstrating their expression in COS-1 cells. An extra, high molecular weight band was observed with the N-myc NAT2. This may reflect a mobility shift due to an unknown factor interacting with the cytoplasmic c-*myc* epitope or modification of the N-myc NAT2 product. The presence of this band was insensitive to hydrolysis by endoglycosidase H and *N*-glycosidase F (not shown), suggesting glycosylation was not involved.

The transfected cells were used for indirect immunofluorescent labeling with FITC-conjugated goat anti-mouse IgG. Cells were incubated in the presence or absence of Triton X-100 to compare intracellular and cell surface staining patterns. In the permeabilized mock cells, some background staining can be seen in nuclei (Fig. 5*B*), which may be due to the endogenous c-*myc* protein. Fluorescence was visible in the internal membranes (*i.e.* endoplasmic reticulum and Golgi) and plasma membrane in both of the permeabilized N- and C-terminal tagged NAT2 transfected cells (Fig. 5, *D* and *F*). For the unpermeabilized cells, however, only the C-terminal epitope-tagged protein was detected on the cell surface (Fig. 5*E*), indicating the C terminus is oriented on the outside of the plasma membrane. In contrast, the N-terminal epitope was not detected in unpermeabilized cells (Fig. 5*C*). These data provide additional evidence that the N terminus of NAT2 is inside the cell and the C terminus is outside. Thus, the results of immunofluorescent staining in COS-1 cells further support the 11 transmembrane domain model.

DISCUSSION

In the results presented here, we showed that the N terminus of NAT2/AAP1 is on the cytoplasmic side of the plasma

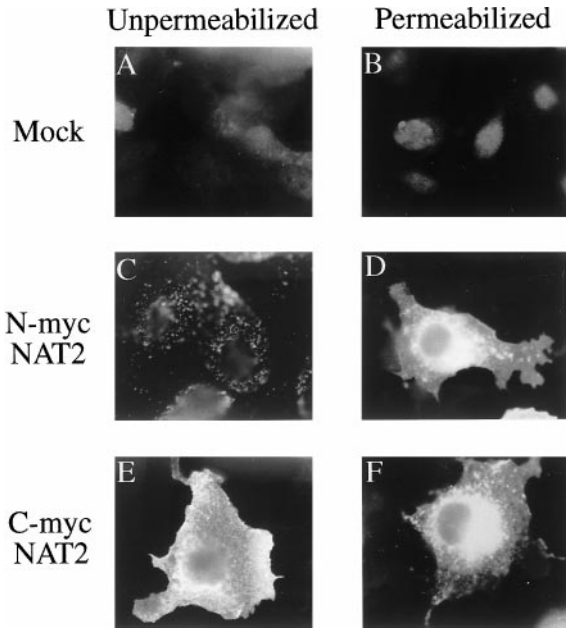

FIG. 5. **Immunofluorescent localization of c-*myc* epitope-tagged NAT2 in COS-1 cells.** COS-1 cells transfected with N- and C-myc NAT2 DNA in pCMV5 expression vector and NAT2 expression were visualized with indirect immunofluorescent labeling. Permeabilized cells were generated by treatment with 0.1% Triton X-100. Proteins were detected with Myc1–9E10 monoclonal antibody as primary and FITC-conjugated goat anti-mouse IgG as secondary antibody. *Panels A, C*, and *E* are unpermeabilized cells; *panels B, D*, and *F* represent permeabilized cells. *Panels A* and *B* are mock cells (transformed with pCMV5 vector only); *panels C* and *D* represent *myc* tagged on the N terminus of NAT2; *panels E* and *F* are *myc*-tagged on the C terminus of NAT2.

membrane, and the C terminus faces outside the cell. This conclusion was supported by the differential sensitivity to proteolysis by the N- and C-terminally tagged NAT2 proteins and by immunofluorescent localization of epitope-tagged NAT2 in COS-1 cells. In addition, partial proteolysis of the *in vitro* translated C-terminal tagged protein produced six immunoprecipitable peptide fragments, suggesting NAT2 has six protein domains that are accessible to proteinase K. An 11-TMD model of NAT2 is proposed based on the number and size of the proteolytic fragments, predictions derived from hydropathy analysis, the absence of protein glycosylation, and localization of the N and C termini of NAT2 on opposite sides of the plasma membrane. Taken together, we believe these data provide good evidence that NAT2 contains 11 TMD.

The novel 11 transmembrane domain model we propose here is different from the well-known model of the major facilitator superfamily that contains a common structural motif of 12 transmembrane segments with cytoplasmic N and C termini (34–37). This superfamily contains many plasma membrane transport systems identified in bacteria, fungi, plants, and animals. Major facilitator superfamily members function as uniporters, symporters, and antiporters for a variety of organic and inorganic substrates (34–39). NAT2 is also unique when compared with the cotransporter family of fungal and bacterial amino acid transporters, which show significant sequence similarity across the prokaryotic-eukaryotic boundary (40, 41). This family contains HIP1 (28), CAN1 (42), PUT4 (43), GAP1 (44), LYP1 (45), and TAT1 and TAT2 (46) in *S. cerevisiae*; and lysP (47), aroP (48), and pheP (49) in *E. coli*. The amino acid carriers in this family exhibit very similar hydrophobic profiles that are predicted to have 12 transmembrane domains (40, 41). Indeed, the topology of lysP in *E. coli* was shown by gene-fusion analysis to have 12 transmembrane domains (50). The distantly related amino acid transporters of animals, such as the family of Na^+-dependent amino acid neurotransmitters (51) and the Na^+-independent cationic amino acid transporters (MCATs) (52) are also predicted to have 12 membrane-spanning regions.

The difference between the 12- and 11-transmembrane topology is the localization of the N and C termini on either face of the plasma membrane. The C terminus of several transport proteins has been implicated in regulating transport activity (53, 54) and in protein processing (55). Interestingly, a C-terminal deletion of NAT2/AAP1 increases transport activity of this porter.[3] Although the reason for this stimulation is still under investigation, this observation suggests that the C terminus may play an important role in transport function. Since the C terminus of NAT2/AAP1 is localized on the outside face of the plasma membrane, this observation also raises the possibility that this carrier could be regulated by extra-cellular factors. NAT2 is also unique when compared with other *Arabidopsis* amino acid transporters such as ProT1, ProT2 (proline transporter; Ref. 18), and AAT1 (cationic amino acid transporter; Ref. 19). So far, the 11-transmembrane topology is specific to the *Arabidopsis* AAP family.

An alignment of the hydropathy profile of the AAP family members shows that they are super-imposable (32). This observation supports our focus on NAT2 as a prototypical example of this family. Interestingly, there is a hyper-variable region between TMD5 and TMD6 of the alignment. According to the topology model, this region is oriented to the outside of the cell. This observation raises the interesting hypothesis that this loop may be involved in defining substrate specificity. When we compare the amino acid sequences in this region, some members contain similar numbers of charged amino acid residues. For example, AAP2 and AAP4 have three basic amino acid residues, and they transport the same group of amino acids. Likewise, AAP3 and AAP5 share significant similarities in both charge and substrate patterns (17, 18). The importance of these observations will require additional investigations.

As a growing number of amino acid transporters are identified in higher plants, it becomes increasingly important to define the molecular characteristics of these amino acid transporters in the context of nitrogen allocation across the plant as a multicellular organism. The topology of NAT2/AAP1 described here is the foundation of future investigations of the structure and function of the *Arabidopsis* AAP family.

Acknowledgments—We thank Dr. N. V. Raikhel (Michigan State University, East Lansing, Michigan) for providing the 6x-*myc* cassette, Dr. E. Szczesna-Skorapa and Ci-Di Chen (Department of Molecular and Integrative Physiology, University of Illinois) for discussing the *in vitro* transcription/translation experiments and help with COS-1 cell transfection and indirect immunofluorescence.

REFERENCES

1. Bush, D. R. (1993) *Annu. Rev. Plant Physiol. Plant Mol. Biol.* **44,** 513–542
2. Briskin, D. P. (1990) *Biochem. Biophys. Acta* **1019,** 95–109
3. Serrano, R. (1989) *Annu. Rev. Plant Physiol. Plant Mol. Biol.* **40,** 61–94
4. Pate, J. S. (1983) in *Plant Physiology: A Treatise, Vol. VIII: Nitrogen Metabolism.* (Stewart, F. C. and Bidwell, R. G. S., eds) pp. 335–401, Academic Press, New York
5. Bush, D. R. (1998) in *Plant Amino Acids: Biochemistry and Biotechnology.* (Singh, B., ed) Marcel Dekker, NY, in press
6. Li, Z.-C., and Bush, D. R. (1990) *Plant Physiol.* **94,** 268–277
7. Bush, D. R., and Li, Z.-C. (1991) in *Recent Advances in Phloem Transport and Assimilate Compartmentation*. (Bonnemain, J. L., Delrot, S., Lucas, W. J., and Dainty, J., eds) pp. 148–153, Presses Academiques, France
8. Li, Z.-C., and Bush, D. R. (1991) *Plant Physiol.* **96,** 1338–1344
9. Li, Z.-C., and Bush, D. R. (1992) *Arch. Biochem. Biophys.* **294,** 519–526
10. Williams, L. E., Nelson, S. J., and Hall, J. L. (1990) *Planta* **182,** 540–545
11. Williams, L. E., Nelson, S. J., and Hall, J. L. (1992) *Planta* **186,** 541–550
12. Boorer, K. J., Frommer, W. B., Bush, D. R., Kreman, M., Loo, D. D. F., and Wright, E. M. (1996) *J. Biol. Chem.* **271,** 2213–2220

[3] L. Chen and D. R. Bush, unpublished data.

13. Hsu, L.-C., Chiou, T.-J., Chen, L., and Bush, D. R. (1993) *Proc. Natl. Acad. Sci. U. S. A.* **90,** 7441–7445
14. Frommer, W. B., Hummel, S., and Riesmeier J. W. (1993) *Proc. Natl. Acad. Sci. U. S. A.* **90,** 5944–5948
15. Tanner, W., and Caspari, T. (1996) *Annu. Rev. Plant Physiol. Plant Mol. Biol.* **47,** 595–626
16. Kwart, M., Hirner, B., Hummel, S., and Frommer, W. B. (1993) *Plant J.* **4,** 993–1002
17. Fischer, W.-N., Kwart M., Hummel, S., and Frommer, W. B. (1995) *J. Biol. Chem.* **270,** 16315–16320
18. Rentsch, D., Hirner, B., Schmelzer, E., and Frommer, W. B. (1996) *Plant Cell* **8,** 1437–1446
19. Frommer, W. B., Hummel, S., Unseld, M., and Ninnemann, O. (1995) *Proc. Natl. Acad. Sci. U. S. A.* **92,** 12036–12040
20. Chen, L., and Bush, D. R. (1997) *Plant Physiology* **115,** 1127–1134
21. Bush, D. R., Chiou, T.-J., and Chen, L. (1996) *J. Exp. Bot.* **47,** 1205–1210
22. Kunkel, T. A. (1985) *Proc. Natl. Acad. Sci. U. S. A.* **82,** 488–492
23. Evan, G. I., Lewis, G. K., Ramsay, G., and Bishop, J. M. (1985) *Mol. Cell. Biol.* **5,** 3610–3616
24. Sauer, N., and Stolz, J. (1994) *Plant J.* **6,** 67–77
25. Andersson, S., Davis, D. N., Dahlback, H., Jornvall, H., and Russell, D. W. (1989) *J. Biol. Chem.* **264,** 8222–8229
26. Sambrook, J., Fritsch, E. F., and Maniatis, T. (1989) *Molecular Cloning: A Laboratory Manual*, 2nd Ed., Cold Spring Harbor Laboratory, Cold Spring Harbor, NY
27. Sanger, F., Nicklen, S., and Coulson, A. R. (1977) *Proc. Natl. Acad. Sci. U. S. A.* **74,** 5463–5467
28. Tanaka, J. I., and Fink, G. R. (1985) *Gene* **38,** 205–214
29. Becker, D. M., and Guarente, L. (1991) *Methods Enzymol.* **194,** 182–187
30. Lively, M. O., and Walsh K. A. (1983) *J. Biol. Chem.* **258,** 9488–9495
31. Szczesna-Skorupa, E., and Kemper, B. (1993) *J. Biol. Chem.* **268,** 1757–1762
32. Kyte, J., and Doolittle, R. F. (1982) *J. Mol. Biol.* **157,** 105–132
33. Maddy, A. H. (1976) *J. Theor. Biol.* **62,** 315–326
34. Griffith, J. K., Baker, M. E., Rouch, D. A., Page, M. G. P., Skurray, R. A., Paulsen, I. T., Chater, K. F., Baldwin, S. A., and Henderson, P. J. F. (1992) *Curr. Opin. Cell Biol.* **4,** 684–695
35. Henderson, P. J. F. (1993) *Curr. Opin. Cell Biol.* **5,** 708–721
36. Marger, M. D., and Saier, M. H., Jr. (1993) *Trends. Biochem. Sci.* **18,** 13–20
37. Goswitz, V. C., and Brooker, R. J. (1995) *Protein Sci.* **4,** 534–537
38. Muchhal, U. S., Pardo, J. M., and Raghothama, K. G. (1996) *Proc. Natl. Acad. Sci. U. S. A.* **93,** 10519–10523
39. Smith, F. W., Ealing, P. M., Dong, B., and Delhaize, E. (1997) *Plant J.* **11,** 83–92
40. Sophianopoulou, V., and Diallinas, G. (1995) *FEMS Microbiol. Rev.* **16,** 53–75
41. Andre, B. (1995) *Yeast* **11,** 1575–1611
42. Hoffmann, W. (1985) *J. Biol. Chem.* **260,** 11831–11837
43. Vandenbol, M., Jauniaux, J.-C., and Grenson, M. (1989) *Gene* (*Amst.*) **83,** 153–159
44. Jauniaux, J.-C., and Grenson, M. (1990) *Eur. J. Biochem.* **190,** 39–44
45. Sychrova, H., and Chevallier, M. R. (1993) *Yeast* **9,** 771–782
46. Schmidt, A., Hall, M. N., and Koller, A. (1994) *Mol. Cell. Biol.* **14,** 6597–6606
47. Steffes, C., Ellis, J., Wu, J., and Rosen, B. P. (1992) *J. Bacteriol.* **174,** 3242–3249
48. Honore, N., and Cole, S. T. (1990) *Nucleic Acids Res.* **18,** 653
49. Pi, J., Wookey, P. J., and Pittard, A. J. (1991) *J. Bacteriol.* **173,** 3622–3629
50. Ellis, J., Carlin, A., Steffes, C., Wu, J., Liu, J., and Rosen, B. P. (1995) *Microbiology* **141,** 1927–1935
51. Clark, J. A., and Amara, S. G. (1993) *Bioessays* **15,** 323–332
52. Kavanaugh, M. P., Wang, H., Zhang, Z., Zhang, W., Wu, Y.-N., Dechant, E., North, R. A., and Kabat, D. (1994) *J. Biol. Chem.* **269,** 15445–15450
53. Dauterive, R., Laroux, S., Bunn, R. C., Chaisson, A., Sanson, T., and Reed, B. C. (1996) *J. Biol. Chem.* **271,** 11414–11421
54. Palmgren, M. G., Sommarin, M., Serrano, R., and Larsson, C. (1991) *J. Biol. Chem.* **266,** 20470–20475
55. Olivares, L., Aragon, C., Gimenez, C., and Zafra, F. (1994) *J. Biol. Chem.* **269,** 28400–28404